STUDY OF OXIDATION KINETICS OF Al-Si ALLOYS WITH HIGH CONCENTRATION OF IMPURITIES (Fe, Zr, V)

Anna Petrova[1]* ID, Svetlana Yaneva[2] ID, Adelina Miteva[1], Georgi Stefanov[2] ID, Boris Barbov[3]

[1]Space Research and Technology Institute, Bulgarian Academy of Sciences, Bulgaria
[2]Institute of Metal Science, Equipment and Technologies with Hydro- and Aerodynamics „Acad. A. Balevski", Bulgarian Academy of Sciences, Bulgaria
[3]University of Oxford, United Kingdom

Abstract:

Aluminium alloys are used as lightweight materials especially in the aerospace and automotive industries. They have a number of properties such as high corrosion resistance due to the surface oxide coating, low relative weight and better castability. At normal temperatures, metal oxides are more resistant than the metal itself. The oxide layer is much thinner than the metal but protects it from interacting with the air. The kinetics of oxidation processes is the subject of the current work. As the temperature rises, the oxidation process usually proceeds in the presence of water vapour, and its rate depends on various factors, including the initial oxide layer and oxidation kinetics. The values of the oxidation exponent *n* are calculated for aluminium ribbons with different contents of Fe, Mg and Sb. Their influence on the intensity and two-stage tendency of the oxidation process is established.

1. INTRODUCTION

The world amount of aluminium used today is about 80 kg per person [1]. The recycling of Al is carried out by remelting aluminium scrap, whereby depending on the technology from 1 to 15% of the starting material is lost in the form of oxides. In the melting process, aluminium reacts with the gases contained in the atmosphere and oxidizes. The loss of Al from the oxidation of the melt is over 5% [2].

With the application of the rapid solidification of aluminium alloys with a solidification speed of 10^{5-6} K/min it becomes possible to obtain multicomponent aluminium alloys (8-10 wt.% Fe). These are produced for the aerospace industry and have economic significance [3, 4]. This is the basis of the rapid development of nano-microcrystalline alloys.

Aluminium interacts with air and water vapor from it, forming a dense oxide layer. The oxide coating on pure aluminium is only a few μm thick as seen in Fig. 1, but protects the surface from subsequent oxidation. The metal does not react with water even at boiling temperatures. Oxidation is a type of metal corrosion.

The crystallographic forms of the oxide layer on aluminium and its alloys are different, depending on temperature and time. The initial oxide is amorphous, and when heated crystallizes in several crystalline modifications, which changes the mechanism of oxidation.

The main impurities found in cast aluminium alloys are Fe, Mg, Mn, Cu and Zn. With some of them, aluminium forms intermetallic phases. All inclusions whether in the oxide layer or inside the metal, degrade the mechanical properties,

---

*CONTACT: A. Petrova, e-mail: ani@phys.bas.bg

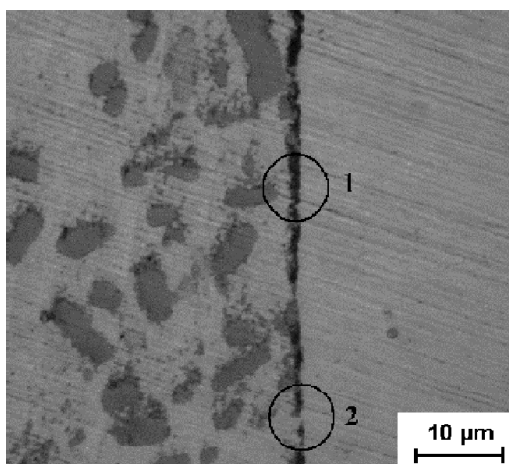reducing the effective cross-section of the metal and its ductility.

Fig. 1. Oxide layer on Al-Si alloy: Area 1 - thick layer and Area 2 - an interruption in the layer

The oxidation kinetics of aluminium and its alloys are affected by a number of surface processes where stable coatings are formed, consisting essentially of aluminium oxide Al_2O_3 equation (1). The formation of Al_2O_3 on the metal surface is accompanied by the penetration of hydrogen deep into the metal.

At high temperatures, the oxidation process takes place in the presence of water vapor involved in the process (Fig. 2).
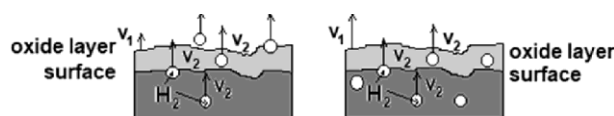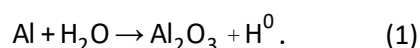

Fig. 2. Scheme of hydrogen porosity growth: a) The material is degasses; b) Pores inside the alloy, where V_1 is the speed of the crystallization front and V_2 is the speed of the bubbles or the rate of diffusion of hydrogen

The oxidation of aluminium and its alloys [5, 6] is the result of the reaction of aluminium with water vapor according to the reaction:

$$Al + H_2O \rightarrow Al_2O_3 + H^0. \qquad (1)$$

The different kinetic dependences of the oxidation of aluminium and its alloys are, compared according to basic models, demonstrated by the dependence of the increase in the specific weight of the oxide layer W over time t [7]. The kinetic data for most aluminium alloys is represented by the function:

$$W^n = k_j(t_i + t_0) + \text{const}, \qquad (2)$$

where n is an exponent, t_i - oxidation time, the time t_0 [s] is an incubation period, which is relatively short. The incubation period t_0 of equation (2) is zero if the weight measurement starts with start of heating as it was with our experiments. Basic values of the parameter n are observed.

The index n is equal to 1 when the dependence is linear. Usually the linear increase of the oxidative coating over time is characteristic of for the initial moments of the process and of the oxidation process at low temperatures.

The exponent is equal to 2. Parabolic dependence describes the formation of a compact oxide layer. The growth of the oxide layer is determined by the diffusion of Al-ions through the layer according to C. Wagner [8]. Values for $n = 2$ are often found in our studies and are associated with obtaining a stable oxide coating in most of the alloys tested.

For values of $n > 2$, an intense increase of the oxide layer is expected [9, 10].

The above shows that, with a wide variety of mechanisms, it is necessary to determine the exponent n (depending on 1), which is taken as the important parameter in determining the mechanism of the oxidation process.

This article compares the results of oxidation testing for various aluminium alloys obtained at the same cooling rates at natural humidity. The aim is to study the kinetics of oxide layer formation on aluminium products and to find ways to control the oxidation process.

2. MATERIALS AND METHODS

The formed ribbons of about 100 μm thickness are obtained by rapid solidification of the melt by the PFC method. At the same time microcrystalline powders with a particle size of about a few μm are also obtained by atomization of the melt. Two kind of nano-micro materials were received: ribbons and particles. After rapid solidification of the melt, cold compacting (300 °C) and consistent hot extrusion (450 - 480 °C) high density solid specimens are obtained from the loose materials. In both cases, the aluminium alloys are subjected to high temperatures and the oxidation process can be intense.

Fig. 3 shows a cold precompacted powder sample of Al-Fe-Si-V alloy. The figure shows visible after cold compacting of the oxide layer on the particles. It is necessary to increase the force and also the temperature during the extrusion to

merge the particles into a single alloy. This difference in the requirements for the oxide layer necessitates the study of the oxidizing process and finding the optimal temperature conditions for obtaining quality workpieces.
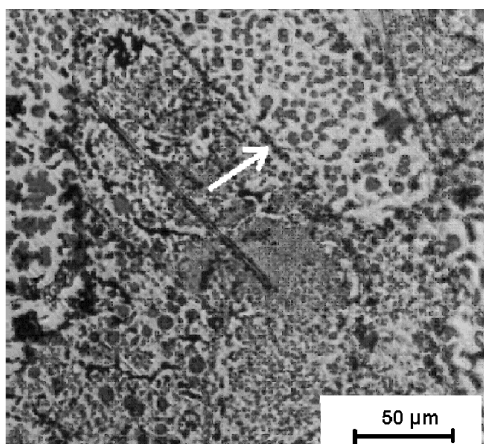

Fig. 3. Microstructure of cold compacted sample

The studied Al-Si nano-microcrystalline alloys contain different alloying elements as shown in Table 1.

Table 1. Chemical composition of the alloys, wt. %

Ribbon	Fe	Si	Mg	Sb	Al
1 Basic	0.25	11.50	-	-	88.25
2 Alloy with an increased Fe content	2.00	12.10	0.20	-	85.70
3 Alloy with an increased Fe content	2.52	11.70	0.20	-	85.58
4. Alloy with Sb and an increased Fe content	2.22	12.2	-	0.17	85.41
5. Alloy with an increased Mg content	0.32	11.75	0.61	-	87.32
6. Alloy with Sb	0.20	11.00	-	1	87.80

The data obtained by us are processed by the following procedure: the dependence on equation (2) after logarithm:

$$n \ln W = \alpha \ln t \qquad (3)$$

$$n = \frac{\alpha \ln t}{\ln W} \qquad (4)$$

Where a is a parabolic constant. The data are processed by the least squares method. Such a process may imply a uniform diffusion of one or more of the reactants through a growing layer.

A least-squares method of calculations was conducted to find the most expected curves.

A standard χ^2 (chi squared) test was used to test the quality of the fitting.

To determine n, calculate χ^2 of formula:

$$\chi^2 = \sum_{i=1}^{10} \left(\frac{W_i(t) - W_i(\exp)}{0.1 . W_i(\exp)} \right)^2 \qquad (5)$$

where W_i are the experimental points.

The oxidation of the samples is carried out with the help of thermal balance „Setaram" of relative sensibility 4.10^{-8} g and stability 1.10^{-6} g in air at 550 °C for a time of 120 min.

Due to the resistance of the oxide coatings to the ribbons, it was necessary to raise the oxidation temperature to 550 °C for kinetic studies, where quantitative measurement of the process speed is possible. At this temperature, the law of increase of the oxide layer of Al and the alloys is quadratic. This law is typical of most aluminium alloys (Fig. 4), which have an aluminium solid solution as a separate phase [11].
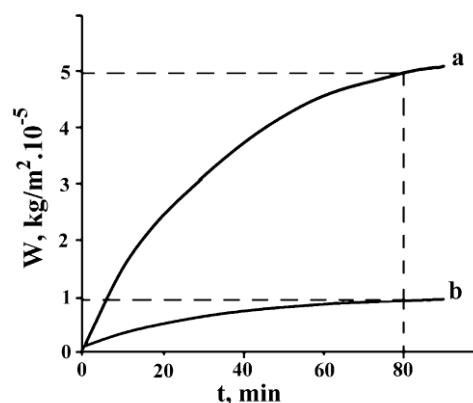

Fig. 4. Weigth-gain-time curves of (a) Al-Si bulk alloy and (b) ribbon

Fig. 4 shows the oxidation curves for a sample of Al-9.5Si-1.38Zr alloy in two variants: a nano-microcrystalline ribbon (b) and an initial solid alloy (a). As can be seen from the figure, the oxidation curve of the nano-microcrystalline ribbon is significantly lower than that of the original solid alloy. Fast curing also provides a significant reduction in oxidation compared to the parent casting alloy.

3. RESULTS AND DISCUSSION

To identify the oxidation processes, a method for determining the constants in equation (2) is introduced. We chose alloy B (Al-10Fe-2.7V-10Si).

In order to calculate the exponent *n* by using equation (2), the weight changes *W*, [kg/m^2], were plotted against the oxidation time *t*, [s] in logarithmic coordinates and linear regression analyzes have been done. Fig. 5 shows such dependencies for ribbon B.

At a constant temperature with increasing oxidation time, *n* changes its value (Fig. 5 b). The dependence of *n* on time is shown by two lines intersecting for *n* = 4.

Through logarithm, phase transitions are demonstrated with different straight lines that intersect at one point (3.93; 1.06), ribbon B (Al-10Fe-2.7V-10Si), Fig. 5 (b).

As it is known, complex alloys with high Fe content show complicated behavior in increasing temperatures [12, 13]. In addition to increasing the oxide layer, these alloys exhibit a two-step decomposition of the saturated aluminium solution obtained by rapid crystallization.
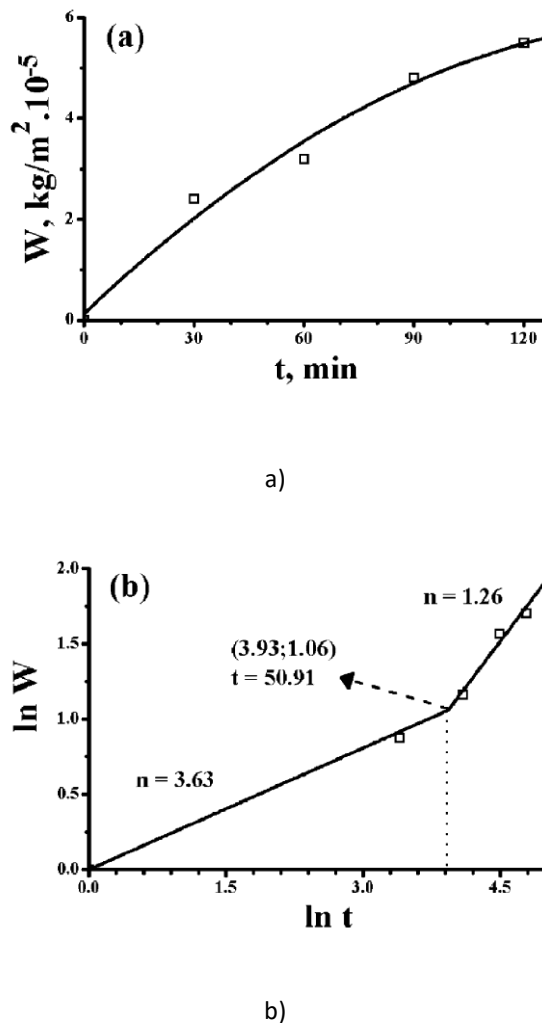
Fig. 6 allows the indication of phase transitions, which are characteristic of high alloy nano-microcrystalline alloys.

We associate the first line in the logarithmic line of ribbon B (Al-10Fe-2.7V-10Si) with the first stage in the formation of the microstructure, during which the saturated solid solution decomposes with the increase of the silicon phase. In the second stage, there is a spontaneous increase in the Fe phases that disrupt the integrity of the oxide coating. The two steps in forming the structure upon heating the nano-microcrystalline ribbons are demonstreted in Fig. 6. The figure shows the DSC curve for isothermal heating of ribbon 3 (with 2.52 wt. % Fe from Table 1).

Two exothermic peaks of different sizes are observed. The first peak is at 274.0 °C and is associated with the breakdown of the saturated solid solution and the increase of the silica particles. The second peak is at 369.6 °C and we associate it with the secondary increase of the Fe containing phases of the aluminium matrix.
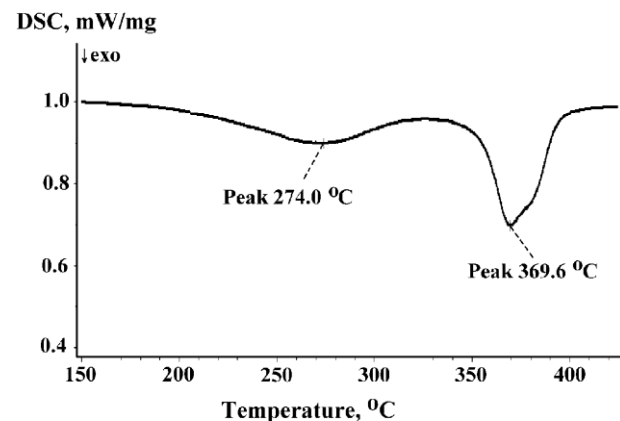

a)

b)

Fig. 5. Ribbon B (Al-10Fe-2.7V-10Si): a) Isotherm *W*(*t*) and b) Linear dependence ln *W*/ln *t*

Fig. 6. DSC-experimental curve for ribbon 3 (2.52 wt. % Fe)

Rapid solidification allows to receive alloys with high Fe content without large intermetallic phases (peculated for these alloys [14]) and with low oxidation possibility. It was possible to produce many alloys with high Fe and good quality.

To study the kinetics of oxidation, Barbov and Petrova [15] developed a program for calculating by criterion χ^2 in the statistical processing of experimental data (Fig. 7). Until now, we have calculated the values of *n* through logarithm of experimental data on equation (2). The values for *n* are found from the slope of the most probable line

by the least squares method. To speed up the process, we have developed a program for calculating the criterion χ^2 for the statistical processing of experimental data by PC.

The methodology for calculation of n has been applied to many nano-microcrystalline alloys obtained by us (Table 1). Some of these results are shown in Table 2. As can be seen from the table, the alloys studied show values for $n \geq 2$. The parameter $n = 2$ is characteristic of „pure" Al-Si alloys, without micro- and macronutrients. As shown in [9], the oxide layer in such alloys is dense and in the process of heating the layer covers the silica particles without interruption. Some other elements added to Al-Si alloys influence the oxidation kinetics. Such element is Mg. As in many Al-Si alloys [16], Mg is added to improve the heat treatment conditions. Mg accelerates oxidation of Al-Si alloys. In the Table 2 the highest value for $n = 4.7$ is for ribbons with the highest Mg concentration. As it is shown in Table 2 values of n change with the addition of the different element: Al-Si alloys with high concentration Fe < „pure Al-Si" < Al-Si (0.6 % Mg).

The intensity of the oxidation process is also associated with a disruption of the integrity of the oxide layer and a new direct access of oxygen to the metal surface. Fig. 1 shows the rupture of the oxide layer. Despite the formation of Fe containing phases, nano-microcrystalline alloys with a high Fe content show a decrease in the rate of oxidation.

Table 2 compares the calculated values exponent n, obtained by different methodologies for basic ribbon 1.
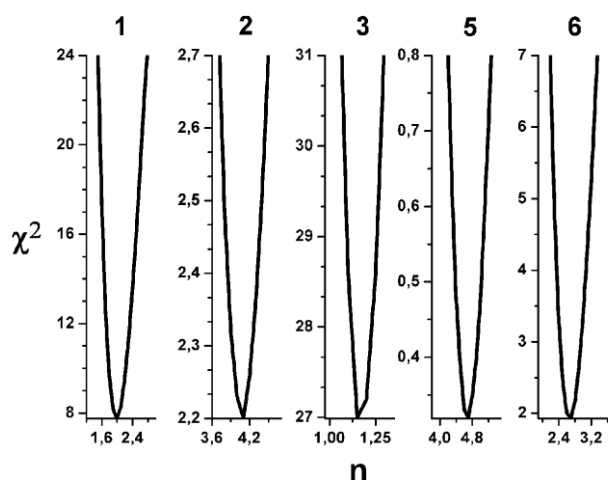
Table 2. Comparison of values of n obtained by different methods

Aluminium alloys	Exponent n by χ^2	Fe, wt. %
Basic ribbon 1	2.02	0.25
	2.00 by calculation in [15]	
	2.21 by calculation in [9]	
Ribbon 2	4.1	2.00
Ribbon 3	1.17	2.52
Ribbon 4	0.6	2.22
	1.18	
Ribbon 5	4.7	0.32
Ribbon 6	3.10	0.20
Alloy B	3.63	10
	1.26	
AlFe8VSi2 550 °C	2.27	8-10
AlFe8VSi2 585 °C	2.86	8-10
AlFe8VSi2 600 °C	2.74	8-10

Rapid solidification also provides a significant reduction in oxidation compared to the initial casting alloy. With the proper rapid solidification and atomization process and subsequent extrusion, the improvement of the microstructure and properties of the alloys obtained is impressive.

The values of n for all the nano-microcrystalline ribbons shown in Table 2 with a high Fe content are close to 1, i.e. the increase of the oxide coating is very slow compared to the alloys where n > 1. This feature of influence of Fe on the oxidation of aluminium alloys is at the base of the production of alloys with enhanced mechanical properties and, as can be seen from our results with the increased oxidation resistance that are applicable to the aerospace industry.

As the temperature increases, the exponent n changes, which indicates that the oxidation rate also changes. It can be concluded that in one chemical composition (the same Mg content), homogeneous distribution of the elements in the sample, the thickening of the structure leads to the formation of a stable oxide layer which covers the all metal surface.

4. CONCLUSIONS

Different kinetic oxidation dependences of aluminium and its alloys can occur in the same metal, in dependence on the conditions of production and operation. Additives of impurity elements even in small concentrations can change the mechanism of oxidation.

Fig. 7. Dependence χ^2 on exponent n for ribbons 1, 2, 3, 5 and 6

1. Accelerated statistical processing of kinetic results using the χ^2 criterion has been developed.

2. Adding Fe to the ribbons changes the grade of $n = 1.2$. Fe is a major alloying element and is present as an impurity in almost all alloys. Due to the rapid solidification, the „harmful" impurity Fe has a beneficial effect, greatly reducing the tendency for oxidation.

3. A major component in many aluminium alloys is Mg. Mg plays a significant role in the oxidation process. In our study, the exponent n is the highest for the alloy containing Mg content 0.61 wt. % in it.

4. The rapid solidification of the alloys helps to reduce the rate of high temperature oxidation by reducing the thickness of the oxide layer 5 times (Fig. 4).

5. Knowledge of the oxidation process allows to take action on minimize the adverse effect of the oxide layer on the structure and properties of the extruded specimens.

6. The calculation of the exponent n, according to the proposed methodology, allows us to suppose phase transitions during in the heating process. Heating leads to a change in the structure, which is associated with a destruction of the oxide coating and a change in the kinetics of oxidation.

In thermo-mechanical treatment, the oxidation of the ribbons forms a thin oxide layer that does not interfere with the process of consolidation by hot extrusion.

Knowledge of the oxidation process allows to minimize the impact of the oxide layer on the sample's structure.

ACKNOWLEDGEMENTS

REFERENCES

[1] Primary Aluminium Production, International Aluminium Institute, London, United Kingdom, 2021.

[2] S.K. Das, Reduction of oxidative melt loss of aluminum and its alloys, DE-FC36-00ID13898. *Secat, Inc.,* 2006.

[3] S. Das, P. Gilman D. Raybould, Applications of rapidly solidified high temperature aluminum alloys. *Key Eng. Mat.*, 1990: 38-39, 367-392.
https://doi.org/10.4028/www.scientific.net/kem.38-39.367

[4] S.P. Nikanorov, V.N. Osipov, L.I. Regel, Structural and mechanical properties of directionally solidified Al-Si alloys. *J. Mat. Eng. and Perf.,* 28, 2019: 7302-7323.
https://doi.org/10.1007/s11665-019-04414-3

[5] V.I. Dobatkin, P.M. Gabidullin, B.A. Kolachev, G.S. Makarov, Gases and oxides in aluminum deformable alloys. *Metallurgiy*a, Moscow, 1976. [in Russian]

[6] P.E. Blackburn, E.A. Gulbransen, Aluminum reaction with water vapor, dry oxygen, moist oxygen and moist hydrogen between 500° and 625°C. *Jornal of The Electrochemical Society*, 107, 1960: 944-950.
https://doi.org/10.1149/1.2427576

[7] V.I. Nikitin, Calculation of heat resistance of metals. *Metallurgiya*, Moscow, 1976. [in Russian].

[8] C. Wagner, The distribution of cations in metal oxide and metal sulphide solid solutions formed during the oxidation of alloys. *Corrosion Science*, 9(2), 1969: 91-109.
https://doi.org/10.1016/S0010-938X(69)80046-6

[9] S. Yaneva, L. Stojanova, T. Markov, Oxidation of solid aluminium silicon alloys in air. *Cryst. Res. Technol.*, 22, 1987: 251-258.
https://doi.org/10.1002/crat.2170220219

[10] W. Kahl, E. Fromm, Examination of the strength of oxide skins on aluminum alloy melts. *Metall. Trans. B*, 16, 1985: 47-51.
https://doi.org/10.1007/BF02657487

[11] A. Miteva, A. Petrova, G. Stefanov, Surface oxidation of Al-Si alloys at elevated temperatures. *Appl. Eng. Lett*., 6(3), 2021: 105-110.
https://doi.org/10.18485/aeletters.2021.6.3.3

[12] E. Lavernia, J. Ayers, T. Srivatsan, Rapid solidification processing with specific application to aluminium alloys. *Int. Mater*., 37(1), 1992: 1-44.
https://doi.org/10.1179/imr.1992.37.1.1

[13] P. Gilman, M. Zedalis, J. Peltier, S. Das, Rapidly solidified aluminum-transition metal alloys for aerospace applications, *Aircraft Desigh*, 1988, Systems and Operations Conf. Atlanta, USA, AIAA-88-444.

[14] S. Yaneva, A. Kalkanli, K. Petrov, R. Petrov, Ir. Yvan Houbert, S. Kassabov, Structure

development in rapidly solidified Al-Fe-V-Si ribbons. *Materials Science and Engineering*, A 373, 2004: 90-98. https://doi.org/10.1016/j.msea.2003.12.034

[15] B. Barbov, A. Petrova, Oxidation of Aluminum Alloys in the Processing Condition. *14th International Scientific Conference Space,* *Ecology, Safety (SES 2018)*, 7-9 November 2018, Sofia, Bulgaria, 447-450.

[16] S. Yaneva, N. Stoichev, Z. Kamenova, S. Budurov, Quaternary iron-containing phases in Al-Si cast alloys. *Zeitschrift fuer Metallkunde/Materials Research and Advanced Techniques*, 75(5), 1984: 395-398.